Oscillations and synchronization in a system of three reactively coupled oscillators

Alexander P. Kuznetsov[1], Ludmila V. Turukina[1,2],
Nikolai Yu. Chernyshov[3] and Yuliya V. Sedova[1,*]
[1] *Kotel'nikov's Institute of Radio-Engineering and Electronics of RAS, Saratov Branch, Zelenaya 38, Saratov, 410019, Russian Federation*
[2] *Department of Physics and Astronomy, Potsdam University, 14476 Potsdam-Golm, Germany*
[3] *Saratov State University, Astrachanskaya 83, Saratov, 410012, Russian Federation*
(Dated: April 14, 2015)

We consider a system of three interacting van der Pol oscillators with reactive coupling. Phase equations are derived, using proper order of expansion over the coupling parameter. The dynamics of the system is studied by means of the bifurcation analysis and with the method of Lyapunov exponent charts. Essential and physically meaningful features of the reactive coupling are discussed.
*Corresponding author. Tel.:+7 8452278685; fax: +7 8452272401
E-mail address: sedovayv@yandex.ru (Yu.V.Sedova)

PACS numbers: 05.45.-a, 05.45.Xt

arXiv:1503.05313v3 [nlin.CD] 13 Apr 2015

I. INTRODUCTION

Phenomena of synchronization of oscillators are wide spread in nature and technology. A variety of examples can be found in electronics, laser physics, biophysics, chemistry, neuroscience, etc. [1–6]. Synchronization in modern experiments for optomechanical, micromechanical, electronic oscillators is investigated, e.g. see [7–11]. The general picture of oscillatory modes in arrays of elementary oscillators substantially depends on a number of the elements and of the coupling type. In the simplest case of two oscillators with *dissipative coupling* one can observe mutual mode locking of the oscillators with different natural frequencies, two-frequency quasi-periodic oscillations, the effect of "the oscillation death", and the regime called the "broadband synchronization" specific for the oscillatory elements with non-identical control parameters [1–3, 12–16]. With increase of a number of the oscillatory elements the picture becomes more complicated; many features of it have been established and understood recently [17–23].

More complex is a case of *reactive coupling* (termed sometimes as the conservative coupling) [1–3, 13–15]. In radio-engineering and electronics, the coupling of such kind occurs in the case of presence of a reactive element (inductance) in the coupling circuit instead of a resistor giving rise to the dissipative coupling [2]. A topical example of a system with the reactive coupling corresponds to ionic traps [24]. In such traps ions are confined using variable microwave fields, which restrict a magnitude of radial oscillations of the ions, and a constant electric field, limiting the axial motions. In a trap with many electrodes, the ions form a chain being located in the potential wells, and the nonlinearity provides the anharmonic nature of oscillations of the ions in the wells. Additionally, the ions are irradiated by laser beams. The blue laser light of frequency larger than the natural frequency of the ion oscillations provides instability in the system. The red laser light of frequency less than the oscillation frequency gives rise to dissipation. The ions in the chain are coupled due to the Coulomb repulsion. The simplest model of such a system is a chain of reactively coupled van der Pol oscillators [24]. In other concern the models of coupled van der Pol oscillators are studied in application to biological circadian rhythms [25] and for arrays of nanoscale mechanical resonators [26].

The reactive coupling is a phenomenon essentially more subtle than the dissipative coupling. The reason is that when constructing a reduced phase model one must take into account the second order effects in the coupling magnitude. In the case of two oscillators in the first order approximation the coupling effects are generally not manifested. For three or more oscillators the linear terms are present, but the resulting abridged system is conservative [27, 28].

The case of two oscillators was discussed in Refs. [13–15]. There the appropriate model for dynamics of the phase variable was derived and it was shown that the synchronization effect appears only with taking into account the terms of the second order in the coupling parameter. One more feature of the dynamics with the reactive coupling is the phase bistability; it means that depending on initial conditions the oscillators may synchronize either in phase, or in counter-phase. In the present Letter we consider dynamics and synchronization in a chain of three reactively coupled van der Pol oscillators. In contrast to [27, 28], we will assume non-identical oscillators for frequency and focus on the discussion of structure of parameter plane of frequency detuning. The first task is derivation of correct phase equations accounting all relevant effects. Then, they are studied using approaches developed in Refs. [22, 23]. We reveal possible modes of complete and partial synchronization of the oscillators, the bifurcation mechanisms of destruction of the synchronization, and describe arrangement of the parameter domains of quasi-periodic modes with different number

of incommensurable frequencies. One of the main questions we discuss concerns features and distinctions of the reactive coupling in comparison with the earlier known results for the dissipative coupling.

II. THE PHASE MODEL

Consider a set of equations

$$\begin{aligned}
&\ddot{x} - (\lambda - x^2)\dot{x} + x + \varepsilon(x - y) = 0,\\
&\ddot{y} - (\lambda - y^2)\dot{y} + (1 + \Delta_1)y + \varepsilon(y - x) + \varepsilon(y - z) = 0,\\
&\ddot{z} - (\lambda - z^2)\dot{z} + (1 + \Delta_2)z + \varepsilon(z - y) = 0.
\end{aligned} \tag{1}$$

where λ is a parameter controlling intensity of the self-oscillations, Δ_1 and Δ_2 are the detuning parameters for the second and the third oscillators, and ε is the coupling constant.

If the excitation parameter λ is small enough, as well as the detuning parameters, one can apply the slow-amplitude method for the analysis of the equations (1). Using the standard approach [1, 2], one can derive the following equations for the real amplitudes r_i and phases of the oscillators ψ_i (Landau-Stuart equations):

$$\begin{aligned}
&2\dot{r}_1 = r_1 - r_1^3 - \varepsilon r_2 \sin\theta,\\
&2\dot{r}_2 = r_2 - r_2^3 + \varepsilon r_1 \sin\theta - \varepsilon r_3 \sin\varphi,\\
&2\dot{r}_3 = r_3 - r_3^3 + \varepsilon r_2 \sin\varphi,\\
&2\dot{\psi}_1 = \varepsilon - \varepsilon\tfrac{r_2}{r_1}\cos\theta,\\
&2\dot{\psi}_2 = 2\varepsilon + \Delta_1 - \varepsilon\tfrac{r_1}{r_2}\cos\theta - \varepsilon\tfrac{r_3}{r_2}\cos\varphi,\\
&2\dot{\psi}_3 = \varepsilon + \Delta_2 - \varepsilon\tfrac{r_2}{r_3}\cos\varphi.
\end{aligned} \tag{2}$$

Here $\theta = \psi_1 - \psi_2,\ \varphi = \psi_2 - \psi_3$ are relative phases of the oscillators, and the parameters are normalized in respect to the small parameter λ [14, 15]:

$$r \to \sqrt{\lambda} r, \quad t \to t/\lambda, \quad \varepsilon \to \lambda\varepsilon, \quad \Delta \to \lambda\Delta. \tag{3}$$

Subtracting pairwise the phase equations (2), we obtain the following equations for the relative phases:

$$\begin{aligned}
&2\dot{\theta} = -\varepsilon - \Delta_1 + \varepsilon\left(\tfrac{r_1}{r_2} - \tfrac{r_2}{r_1}\right)\cos\theta + \varepsilon\tfrac{r_3}{r_2}\cos\varphi,\\
&2\dot{\varphi} = \varepsilon + \Delta_1 - \Delta_2 + \varepsilon\left(\tfrac{r_2}{r_3} - \tfrac{r_3}{r_2}\right)\cos\varphi - \varepsilon\tfrac{r_1}{r_2}\cos\theta.
\end{aligned} \tag{4}$$

Let us set $r_i = 1 + \tilde{r}_i$, where the tilde designates perturbations of the stationary orbits $r = 1$. The amplitude equations are strongly damped [1, 13–15], so the orbits in a short time reach roughly the stationary amplitudes with some perturbations easily estimated from (2) as

$$2\tilde{r}_1 = -\varepsilon\sin\theta,\ 2\tilde{r}_2 = \varepsilon\sin\theta - \varepsilon\sin\varphi,\ 2\tilde{r}_3 = \varepsilon\sin\varphi. \tag{5}$$

In turn, from the phase equations (4) we obtain

$$\begin{aligned}
2\dot{\theta} = &-\varepsilon - \Delta_1 + 2\varepsilon(\tilde{r}_1 - \tilde{r}_2)\cos\theta\\
&+ \varepsilon(1 + \tilde{r}_3 - \tilde{r}_2)\cos\varphi,\\
2\dot{\varphi} = &\varepsilon + \Delta_1 - \Delta_2 + 2\varepsilon(\tilde{r}_2 - \tilde{r}_3)\cos\varphi\\
&- \varepsilon(1 + \tilde{r}_1 - \tilde{r}_2)\cos\theta.
\end{aligned} \tag{6}$$

Substituting the expressions for the perturbations from (5) we get

$$\begin{aligned}
2\dot{\theta} = &-\varepsilon - \Delta_1 + \varepsilon\cos\varphi - \varepsilon^2\sin 2\theta\\
&+ \varepsilon^2\left(\sin\varphi\cos\theta - \tfrac{1}{2}\sin\theta\cos\varphi + \tfrac{1}{2}\sin 2\varphi\right),\\
2\dot{\varphi} = &\varepsilon + \Delta_1 - \Delta_2 - \varepsilon\cos\theta - \varepsilon^2\sin 2\varphi\\
&+ \varepsilon^2\left(\sin\theta\cos\varphi - \tfrac{1}{2}\sin\varphi\cos\theta + \tfrac{1}{2}\sin 2\theta\right).
\end{aligned} \tag{7}$$

These are the correct phase equations for three reactively coupled oscillators derived up to the terms of order ε^2. Their structure is notably more complex than that for the dissipative coupling [1, 22].

In contrast to the case of two oscillators [13–15], the phase equations (7) do contain terms of the first order in the coupling strength ε, however, for proper description of the synchronization effects these terms are not sufficient. Indeed, if one neglect the quadratic terms, the matrix for perturbations of the stationary state of (7) is

$$\hat{M} = \begin{pmatrix} 0, & -\varepsilon\sin\varphi \\ \varepsilon\sin\theta, & 0 \end{pmatrix}. \tag{8}$$

The trace of this matrix is zero, $S = 0$. It means that a kind of "neutral" state occurs on the border between the stable and unstable solutions (conservative dynamics). Hence, in the system there is no main resonance at all in this approximation. As follows, for description of synchronization phenomena one has necessarily take into account the effects of the second order in the coupling parameter.

Figure 1a illustrates bifurcations of equilibrium points of the system (7). In the case of dissipative coupling the border of the domain of complete synchronization corresponds to a curve of degenerate saddle-node bifurcations, where simultaneous merging occurs for a pair of the saddles with the stable and the unstable nodes [22, 29]. For the reactive coupling the curves of the saddle-node bifurcations SN for merging of a stable node and a saddle and for an unstable node and a saddle do not coincide[33]. Moreover, here a bifurcation of Andronov-Hopf is possible (designated by H), where the equilibrium point becomes unstable with appearance of the stable limit cycle departing from it. Therefore, the region of complete synchronization in the case of reactive coupling of phase oscillators appears to be bounded both by the curves of the saddle-node bifurcations and of the line of the Andronov-Hopf bifurcations. Also we indicate in Figure 1a the points of codimension two: the cusp point CP and the Bogdanov–Takens point BT. In Figure 1b, the domains inside of which system has one or two stable equilibria are shown using different colors. Thus, there is the simplest multistability.

Figure 2 shows the chart of Lyapunov exponents [22, 23] of the system (7) on the parameter plane of frequency detuning of the oscillators (Δ_1,Δ_2). To draw the chart we compute two Lyapunov exponents of the system (7) Λ_1 and Λ_2 at each pixel of the picture and attribute it with a color depending on the signature of the Lyapunov spectrum to visualize the following regimes:

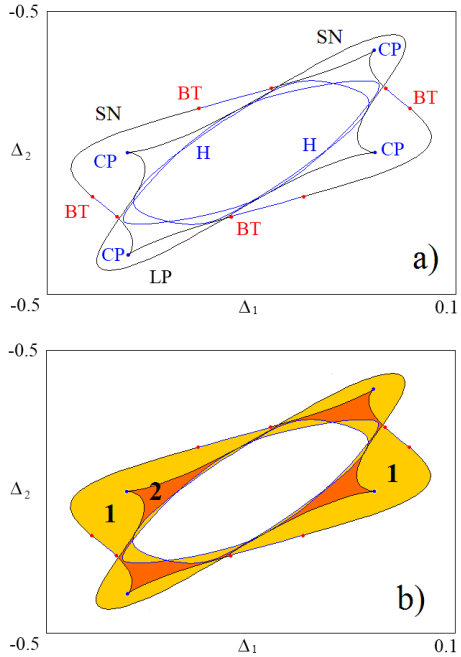

FIG. 1: Bifurcation curves and points of the system (7), $\varepsilon = 0.2$. Digits in fragment b) indicate the number of coexisting stable equilibriums.

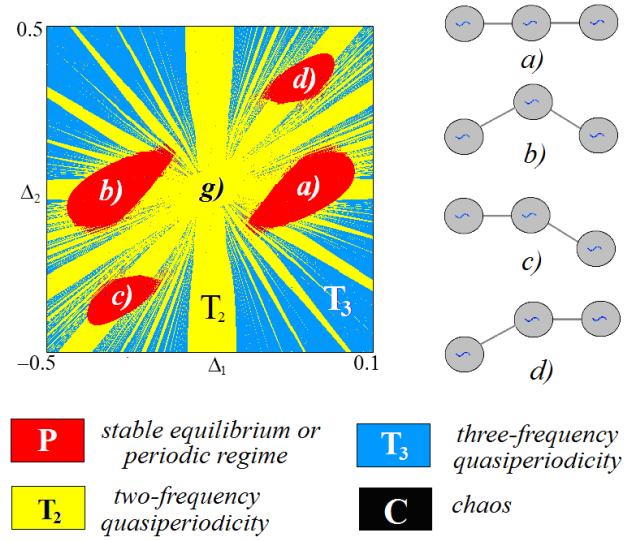

FIG. 2: Chart of Lyapunov exponents on the parameter plane and configurations of basic modes of complete synchronization of the system (7) at $\varepsilon = 0.2$. The letters designate points corresponding to the phase portraits of Fig. 3. Used hereinafter color palette for the Lyapunov charts is shown below.

a) $\Lambda_1 < 0,\ \Lambda_2 < 0$ – the complete synchronization of three oscillators P(red),
b) $\Lambda_1 = 0,\ \Lambda_2 < 0$ – the two-frequency quasi-periodicity T_2 (yellow),
c) $\Lambda_1 = 0,\ \Lambda_2 = 0$ – the three-frequency quasi-periodicity T_3 (blue).
(Here the types of regimes are responsible to original system (1). In this case it is convenient to compare the results obtained at investigations of the phase model and the original system, see Fig.7.)

The area of complete synchronization in Fig. 2 contains four "islands"[34]. In each island we observe a specific kind of complete synchronization as illustrated in the phase portraits of Fig. 3 from (a) to (d). At the point (a) the relative phases are close to zero: $\theta \approx 0$, $\varphi \approx 0$, and this is the synchronization mode of the *in-phase* type. At the point (b) the relative phases are $\theta \approx -\pi$, $\varphi \approx \pi$; so, the first and the third oscillators are roughly in phase while the second oscillator is in the counter-phase relatively to them. This is the *counter-phase* synchronization. In the rest two islands we observe the complete synchronization of *mixed* type. In this case one of the pairs of the oscillators (1-2 or 2-3) are in phase, while the rest is in the counter-phase relative to them. The corresponding configurations of chain are shown in the right part of Fig.2[35].

Beside the region of complete synchronization, on the Lyapunov chart of Fig. 2 one can see a set of bands of two-frequency quasi-periodic regimes immersed in the domain of three-frequency regimes. Within each such band invariant curves of different types occur in the phase plane. Say, in the diagram 3(e) the relative phase of the first and the second oscillators θ fluctuates around a certain equilibrium value, while the phase ϕ varies across the whole range of values. This is *a partial mode-locking of the first and the second oscillators*. In the diagram 3(f) one observes bounded oscillations of the relative phase of the second and thirds oscillators ϕ, so this is *a partial mode-locking of the second and the third oscillators*.

We can classify regions of two-frequency modes with help of the rotation number $w = p : q$. Here p and q are numbers of intersection of the corresponding invariant curve with vertical and horizontal sides of the phase square. Only significant intersections should be used taking into consideration 2π-periodicity of phase. So for Fig.3e the rotation number $w = 0 : 1$ (for both curves) and for Fig.3f $w = 1 : 0$.

This classification becomes obvious if we compute a "torus map" using the numerical calculation of the factors p and q at each point in the parameter plane. The corresponding illustration is given in Fig.4. We use the following rule of coloring. Blue color associates with regime of the rotation number $w = 1 : 0$. Decreasing of the rotation number corresponds to a piecemeal transformation of this color to green mode $w = 1 : 1$. Then green color is gradually transformed into the red for the mode with the rotation number $w = 0 : 1$. Stable equilibriums are shown in white and the other modes – in black. Light gray color corresponds to the regime with contractible limit cycles when invariance curve has no significant intersections with the sides of the phase of a square.

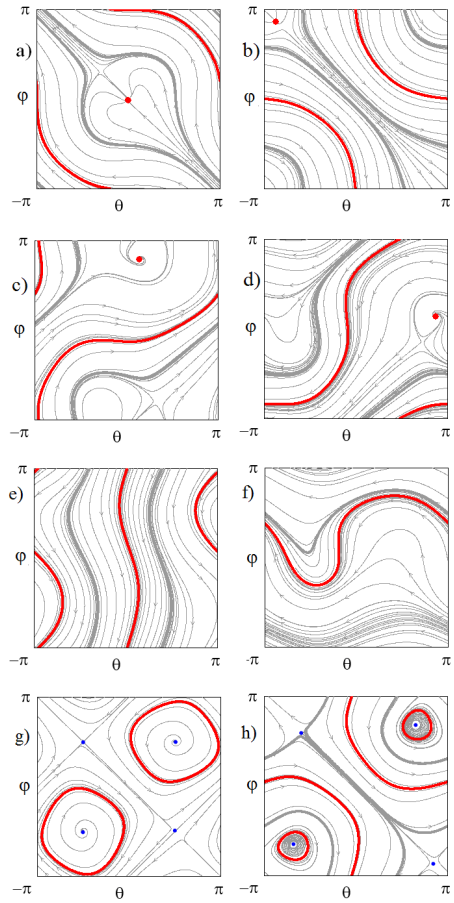

FIG. 3: Phase portraits for the system of three reactively coupled oscillators (7) at $\varepsilon = 0.2$: a) $\Delta_1 = 0$, $\Delta_2 = 0$; b) $\Delta_1 = -0.45$, $\Delta_2 = 0$; c) $\Delta_1 = -0.38$, $\Delta_2 = -0.33$; d) $\Delta_1 = 0$, $\Delta_2 = 0.36$; e) $\Delta_1 = -0.2$, $\Delta_2 = 0.4$; f) $\Delta_1 = 0.05$, $\Delta_2 = 0.22$; g) $\Delta_1 = -0.2$, $\Delta_2 = 0$; h) $\Delta_1 = -0.3$, $\Delta_2 = 0$.

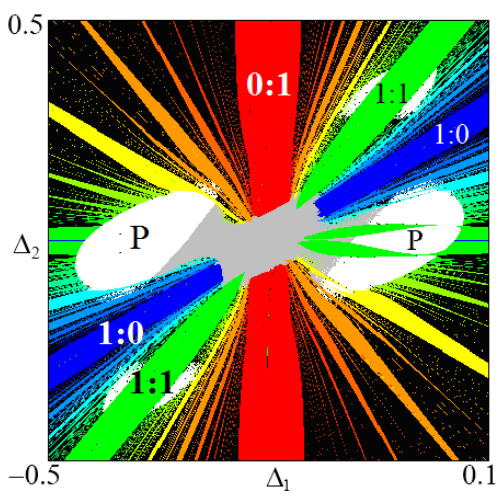

FIG. 4: Map of the two-frequency quasi-periodicity area of the system (7)

Origin of the two frequency bands with a common symmetry center in Figure 2 may be explained by the presence of various possible resonances in the system. To substantiate this point, outline *the partial frequencies* ω_i of the system (6). If we "switch off" in each equation all other oscillators, in the linear approximation we obtain from (6)

$$\omega_1 = \frac{\varepsilon}{2}, \quad \omega_2 = \varepsilon + \frac{\Delta_1}{2}, \quad \omega_3 = \frac{\varepsilon}{2} + \frac{\Delta_2}{2}. \tag{9}$$

A feature of the reactive coupling is that it shifts the partial frequencies by a value of order ε (the shift for the central oscillator is twice as large as for the other ones because it interacts with two rather than one neighbors).

Now, let us write out the main resonances for the partial frequencies. In round brackets the respective conditions are indicated in terms of the frequency detuning parameters:

$$\begin{aligned} &\omega_1 = \omega_2 \ \ (\Delta_1 = -\varepsilon)\,, \\ &\omega_2 = \omega_3 \ \ (\Delta_2 = \Delta_1 + \varepsilon)\,, \\ &\omega_1 = \omega_3 \ \ (\Delta_2 = 0)\,, \\ &\omega_1 + \omega_3 = 2\omega_2 \ \ (\Delta_2 = 2\Delta_1 + 2\varepsilon)\,. \end{aligned} \tag{10}$$

The resonance conditions (10) determine the centers for the wide bands of two-frequency modes in Fig. 2. Additional resonances are possible too, say, $\omega_1 + \omega_2 = 2\omega_3$ etc. They correspond to more narrow bands in Fig. 2. The resonances of higher order give rise to invariant curves with larger number of intersections with the sides of the phase square.

Note that the resonances $\omega_1 = \omega_3$ and $\omega_1 + \omega_3 = 2\omega_2$ determine lines of symmetry on the parameter plane, see Figs. 1 and 2. This is due to symmetry of these resonance conditions in respect to permutation of the first and third oscillators. Say, under the condition $\omega_1 = \omega_3$, i.e. $\Delta_2 = 0$, the equations (7) are transformed one to other under the variable change $\theta \leftrightarrow -\varphi$. As a result, the phase portraits are symmetric about the line $\varphi = -\theta$, see Fig. 3g,h. Analogously, with the condition $\Delta_2 = 2(\Delta_1 + \varepsilon)$ the equations are invariant in respect to the variable change $\theta \leftrightarrow \varphi + \pi$.

A case is interesting of equality of all the partial frequencies $\omega_1 = \omega_2 = \omega_3$ that corresponds to the symmetry center on the parameter plane $\Delta_1 = -\varepsilon$,$\Delta_2 = 0$. The phase portrait at this point is shown in Fig. 3g, and at the point close to it at - in Fig. 3h. In this case invariant curves of other kind arise, which are distinct in their topological properties. The curves in Fig. 3g may be called *contractible*, while those in diagrams (a)-(f) are called *rotational* [31] (for the dissipative coupling the second case is typical [22]). In the first case we have a limit cycle going around the unstable equilibrium point. Then, both the relative phases fluctuate about some mean value. This mode may be characterized as *a partial mode-locking of all three oscillators*. The frequency spectrum produced by the system (1) will contain not only the basic frequency, but also a set of components associated with an additional new time scale, the period

of travel of the representative point around the limit cycle of the phase model.

Contractible limit cycles can occur, as we have already noted, as a result of Andronov-Hopf bifurcation. In addition, the system can demonstrate nonlocal bifurcations when the resulting limit cycle arises from the separatrix loop of the saddle.

Note that several types of multistability are possible in the system with reactive coupling as seen from Fig. 3. Diagrams (a)-(d) correspond to situation when an equilibrium state in the phase space corresponding to the complete synchronization coexists with an invariant curve corresponding to a two-frequency quasi-periodic regime[36]. In diagram (e) two regimes coexist (the in-phase mode and the counter-phase mode) corresponding to partial mode-locking of the first and second oscillators. In turn, in diagram (g) there coexist two regimes of partial synchronization of all three oscillators.

Multistability affects the appearance of the Lyapunov chart. Namely, when choosing different initial conditions one can observe either periodic or quasi-periodic regimes, as can be seen from a comparison of Figures 1 and 2.

III. DYNAMICS OF THE ORIGINAL SYSTEM

Let us illustrate the effectiveness of the phase model. For this purpose we represent the results of the bifurcation analysis of the original system (1) at $\lambda = 0.1$, Figure 5. In accordance with the renormalization rules (3) the coupling parameter $\varepsilon = 0.02$ is selected, which allows to compare Figure 5 for the original system and Figure 1 for the phase model. Now instead of a saddle-node bifurcation of equilibria there is a corresponding bifurcation of limit cycles SNC, instead of the Andronov-Hopf bifurcation - Neimark-Sacker bifurcation NS, and instead of Bogdanov-Takens points - points of 1:1 resonance R1. From Figure 1 and Figure 5 we can see that the Figures are similar to each other, which indicates the effectiveness of the phase model for these values of coupling parameter.

It should be noted that the effectiveness of the phase model will increase with a decrease in the coupling parameter ε. With increasing of coupling parameter its efficiency falls. Fig.6 illustrates this fact, demonstrating bifurcation lines of the phase model and the original system (1). For the phase model we select coupling parameter $\varepsilon = 0.6$, so for original system we have $\varepsilon = 0.06$ (taking into account $\lambda = 0.1$ rescaled on (3)). Some common features - the presence of four lobes - remain. However, the pictures are different in details. Namely, external boundaries of lobes now are mainly the Neimark-Saker lines NS. Lines of saddle-node bifurcations of limit cycles SNC form only small segments of the boundary of complete synchronization area in the vicinity of the cusp points CP associated with bistability areas. One more new feature is the appearance of a double Neimark-Sacker bifurcation points NS-NS.

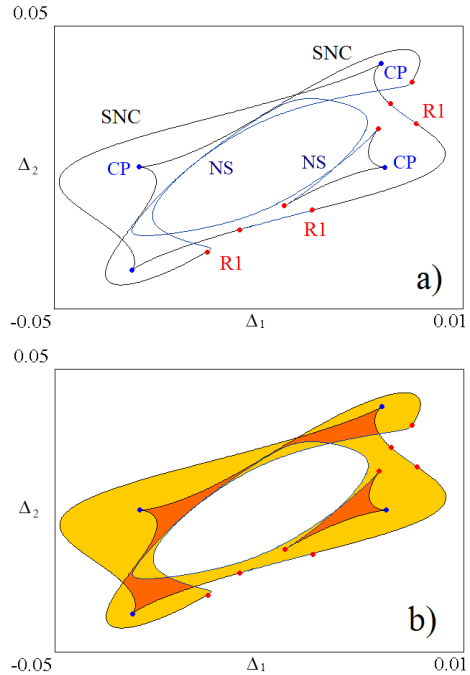

FIG. 5: Bifurcation curves and points of the system (1), $\lambda = 0.1$, $\varepsilon = 0.02$.

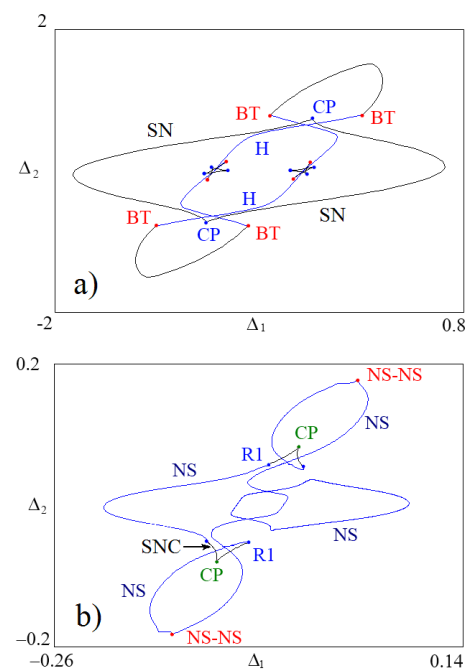

FIG. 6: a) Bifurcation lines and dots of phase model (7), $\varepsilon = 0.6$; b) the similar illustration for the original system (1), $\lambda = 0.1, \varepsilon = 0.06$.

Chart of Lyapunov exponents of the original system (1) is presented in Fig.7 for $\lambda = 0.1, \varepsilon = 0.06$. An enlarged fragment of this chart in Fig.7b should be compared with Fig.6b.

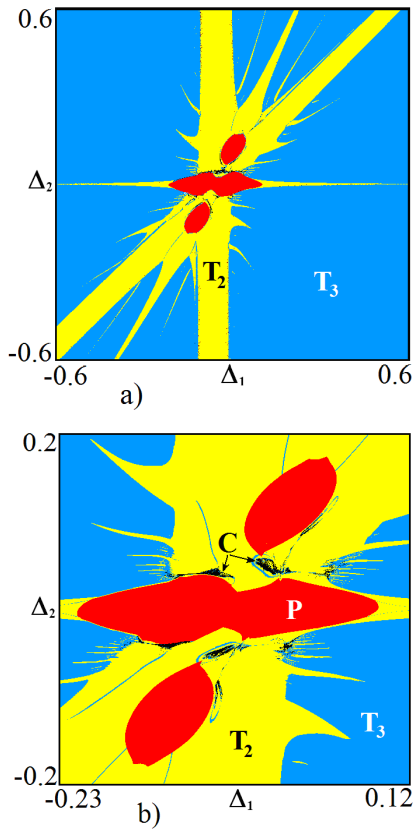

FIG. 7: The chart of Lyapunov exponents and its magnified fragment of the system (1), $\lambda = 0.1, \varepsilon = 0.06$.

With the growth of the λ control parameter both the Landau-Stuart and phase model will work bad to worse. In fig.8a the Lyapunov chart is shown for the system (1) for the case λ=1, ε=0.6. Now the picture is much more complex. Fig.8b shows a new effect: at the intersection of numerous bands of two-frequency modes there are located regions of higher resonances, to which there correspond periodic regimes. This is a characteristic *resonance Arnold web* [32]. Letter D denotes the area of the trajectories' escape to infinity.

IV. CONCLUSION

The results presented here may be of interest for systems such as ion traps [24], biophysical systems [25], etc. At the same time, due to universality of our models, they are important as well in the general theory of synchronization. The main result is that in the description of reactive coupling in the framework of the slow amplitudes approach it is of principal importance to account the effects of the second order in the coupling constant. The region of complete synchronization consists of four "islands" in which the synchronization modes are observed corresponding to in-phase, counter-phase, and mixed types of oscillations in the chain. The bifurcation

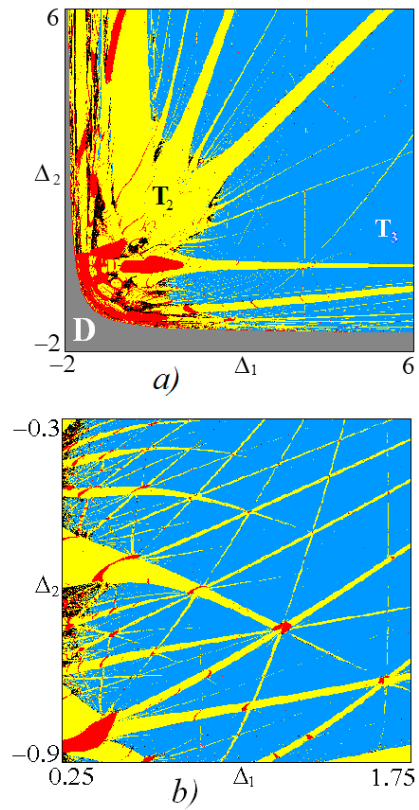

FIG. 8: The chart of Lyapunov exponents and its magnified fragment of the system (1), λ=1, $\varepsilon = 0.6$.

picture of the model formulated in terms of phase variables is significantly different from the case of dissipative coupling. In particular, Andronov – Hopf bifurcation is possible responsible for occurrence of partial synchronization regimes of all three oscillators. For the arrangement of the parameter plane of the frequency detunings, resonances between the partial frequencies are important, and for the reactive coupling the resonance conditions appear to depend on the coupling strength. One more feature is that the quasi-periodic modes of various types can co-exist with complete synchronization, giving rise to many kinds of multistability (coexistence of different attractors).

V. ACKNOWLEDGEMENT

This work was supported by the grants from the President of the Russian Federation for support of leading scientific schools NSH-1726.2014.2 and Russian Foundation for Basic Research project 15-02-02893. Yu.V.S. also thanks Russian Foundation for Basic Research (grant No.14-02-31064).

[1] A. Pikovsky, M. Rosenblum, J. Kurths, Synchronization: A Universal Concept in Nonlinear Science, Cambridge University Press, 2001.

[2] P.S. Landa, Nonlinear Oscillations and Waves in Dynamical Systems, Kluwer Academic Publishers, Dordrecht, 1996.

[3] A.G. Balanov, N.B. Janson, D.E. Postnov, O. Sosnovtseva, Synchronization: from simple to complex, Springer, 2009.

[4] Y. Kuramoto, Chemical Oscillations, Waves, and Turbulence, New York: Springer-Verlag, 1984.

[5] L. Glass, M.C. MacKey, From Clocks to Chaos, Princeton University Press, 1988.

[6] A. Winfree, The Geometry of Biological Time, New York: Springer-Verlag, 2001.

[7] G. Heinrich, M. Ludwig, J. Qian, B. Kubala, F. Marquardt, Collective Dynamics in Optomechanical Arrays, Phys. Rev. Lett. 107 (2011) 043603.

[8] M. Zhang, G. S. Wiederhecker, S. Manipatruni, A. Barnard, P. McEuen, M. Lipson, Synchronization of Micromechanical Oscillators Using Light, Phys. Rev. Lett. 109 (2012) 233906.

[9] A.A. Temirbayev, Y.D. Nalibayev, Z.Z. Zhanabaev, V.I. Ponomarenko, M. Rosenblum, Autonomous and forced dynamics of oscillator ensembles with global nonlinearcoupling: An experimental study, Phys. Rev. E 87 (2013) 062917.

[10] E.A. Martens, S. Thutupalli, A. Fourrière, O. Hallatschek, Chimera states in mechanical oscillator networks, Proc. Natl. Acad. Sci. 110(26) (2013) 10563-10567.

[11] M.R. Tinsley, S. Nkomo, K. Showalter, Chimera and phase-cluster states in populations of coupled chemical oscillators, Nature Phys. 8 (2012) 662-665.

[12] D.G. Aronson, G.B. Ermentrout, N. Kopell, Amplitude response of coupled oscillators, Physica D 41(3) (1990) 403-449.

[13] R.H. Rand, P.J. Holmes, Bifurcation of periodic motions in two weakly coupled van der Pol oscillators // Int. J. Non-Linear Mechanics 15(4-5) (1980) 387-399.

[14] M.V. Ivanchenko, G.V. Osipov, V.D. Shalfeev, J. Kurths, Synchronization of two non-scalar-coupled limit-cycle oscillators, Physica D 189(1-2) (2004) 8-30.

[15] A.P. Kuznetsov, N.V. Stankevich, L.V. Turukina, Coupled van der Pol–Duffing oscillators: Phase dynamics and structure of synchronization tongues, Physica D 238(14) (2009) 1203-1215.

[16] A.P. Kuznetsov, Ju. P. Roman, Properties of synchronization in the systems of non-identical coupled van der Pol and van der Pol–Duffing oscillators. Broadband synchronization, Physica D 238(16) (2009) 1499-1506.

[17] P. Ashwin, J. Guaschi, J.M. Phelps, Rotation sets and phase-locking in an electronic three oscillator system, Physica D 66(3-4) (1993) 392-411.

[18] P. Ashwin, Boundary of two frequency behaviour in a system of three weakly coupled electronic oscillators, Chaos, Solitons and Fractals 9(8) (1998) 1279-1287.

[19] P.S. Linsay, A.W. Cumming, Three-frequency quasiperiodicity, phase locking, and the onset of chaos, Physica D 40(2) (1989) 196-217.

[20] P. Ashwin, O. Burylko, Y. Maistrenko, Bifurcation to heteroclinic cycles and sensitivity in three and four coupled phase oscillators, Physica D 237(4) (2008) 454-466.

[21] Yu. Maistrenko, O. Popovych, O. Burylko, P.A. Tass, Mechanism of desynchronization in the finite-dimensional Kuramoto model, Phys. Rev. Lett. 93 (2004) 084102.

[22] Yu.P. Emelianova, A.P. Kuznetsov, I.R. Sataev, L.V. Turukina, Synchronization and multi-frequency oscillations in the low-dimensional chain of the self-oscillators, Physica D 244(1) (2013) 36-49.

[23] Y.P. Emelianova, A.P. Kuznetsov, L.V. Turukina, I.R. Sataev, N.Yu. Chernyshov, A structure of the oscillation frequencies parameter space for the system of dissipatively coupled oscillators, Communications in Nonlinear Science and Numerical Simulations 19(4) (2014) 1203-1212.

[24] T.E. Lee, M.C. Cross, Pattern formation with trapped ions, Phys. Rev. Lett. 106 (2011) 143001.

[25] K. Rompala, R. Rand, H. Howland, Dynamics of three coupled van der Pol oscillators with application to circadian rhythms, Communications in Nonlinear Science and Numerical Simulation 12(5) (2007) 794-803.

[26] M.C. Cross, A. Zumdieck, R. Lifshitz, J.L. Rogers, Synchronization by nonlinear frequency pulling, Phys. Rev. Lett. 93 (2004) 224101.

[27] A. Pikovsky, P. Rosenau, Phase compactons, Physica D 218(1) (2006) 56-69.

[28] P. Rosenau, A. Pikovsky, Phase compactons in chains of dispersively coupled oscillators, Phys. Rev. Lett. 94 (2005) 174102.

[29] V. Anishchenko, S. Astakhov, T. Vadivasova, Phase dynamics of two coupled oscillators under external periodic force, Europhysics Letters 86(3) (2009) 30003.

[30] A.K. Kryukov, G.V. Osipov, A.V. Polovinkin, J. Kurths, Synchronous regimes in ensembles of coupled Bonhoeffer-van der Pol oscillators, Phys. Rev. E 79 (2009) 046209.

[31] C. Baesens, J. Guckenheimer, S. Kim, R.S. MacKay, Three coupled oscillators: mode locking, global bifurcations and toroidal chaos, Physica D 49(3) (1991) 387-475.

[32] H. Broer, C. Simó, R. Vitolo, The Hopf-saddle-node bifurcation for fixed points of 3D-diffeomorphisms: the Arnol'd resonance web, Bull. Belg. Math. Soc. Simon Stevin 15(5) (2008) 769-787.

[33] In Fig.1 the curves of unstable node bifurcations are not shown to avoid cluttering the figure.

[34] In fact, in accordance with Figure 1b, the regions of complete synchronization are overlapped. On Lyapunov charts this is not visible because of the possibility of multistability in the system.

[35] Analogous modes for coupled Bonhoeffer–van der Pol oscillators were reported in [30].

[36] Actually, Fig.2 is a composition of four charts associated with four variants of the initial conditions and four possible modes of complete synchronization in the system.